Prepared for

Alaska Electric Light & Power

October 2012

Salmon Creek Dam Structural Stability Evaluation

FINAL REPORT

MWH

BUILDING A BETTER WORLD

Salmon Creek Dam
Structural Stability Evaluation
Final Report

TABLE OF CONTENTS

LIST OF TABLES

LIST OF FIGURES

LIST OF APPENDICES

1.0 INTRODUCTION AND BACKGROUND

1.1 Project Background

Salmon Creek Dam, on Salmon Creek, is located in the vicinity of Juneau, Alaska (see **Figure 1**). Salmon Creek enters Gastineau Channel on the Pacific Ocean approximately three miles northwest of downtown Juneau and 2.5 miles downstream of the dam. Salmon Creek Dam was originally built as part of Alaska Gastineau Mining Company's hydroelectric project to produce electricity for mining operations. The dam is now owned by Alaska Electric Light and Power Company (AEL&P).

The first of its kind, Salmon Creek Dam is a constant angle arch designed by Lars Jorgenson, with construction completion in 1914. The dam is 168 feet in height and has a crest length of 642 feet, including a 70-foot section of the spillway on the right abutment. The dam crest elevation is El. 1175 and the spillway crest is at El. 1172. The ungated spillway enters a lined discharge channel before discharging into the creek below beyond the dam's foundation.

Concrete deterioration on the dam faces has been of concern for the last four to five decades. During 1967, the dam underwent a full rehabilitation, which included the following: a drilling and grouting program, removal and repair of deteriorated concrete on the upstream face of the dam between El. 1130-1175 (using a combination of epoxy adhesive and gunite), and removal of spillway gates. The reservoir operating level was restricted to El. 1140 by FERC after a finite element analysis performed in connection with the 1982 FERC Part 12D dam safety inspection determined that the dam may not be stable with a full reservoir level and maximum earthquake. In 2007, a potential failure modes analysis (PFMA) workshop was performed in accordance with Chapter 14 of the FERC Engineering Guidelines, where several potential failure modes (PFMs) were identified and required additional information to categorize (Category III per the Guidelines). These PFMs included failure scenarios resulting from overstressing of the dam due to progressive concrete deterioration or under maximum credible earthquake (MCE) loading. In spring 2011, an investigation program was implemented to gather information for categorization of the PFMs, including a survey using photogrammetric techniques and concrete coring program on the upstream and downstream faces of the dam. The investigation program was aimed at determining the remaining section of the dam, depth of deterioration, and updated concrete strengths.

1.2 Purpose of Project

This seismic stability evaluation is prepared for AEL&P, and follows the 2007 PFMA requirements for Category III PFMs and incorporates the 2011 investigation data. The updated data have been used to develop a finite element model of the dam and to perform an evaluation of dam response to updated earthquake loading.

1.3 Scope of Work

To achieve the objectives of the seismic stability evaluation of Salmon Creek Dam, MWH performed the following tasks:

Task 1: Review of available technical documents for the dam, including:

- Available dam construction records, drawings, correspondence, and photographs.
- Previous seismic hazard analysis.
- Previous Part 12D Dam Safety Reports and Supporting Technical Information Documents.
- Laboratory test results of concrete cores extracted from the dam previously (during 1967 dam rehabilitation) and recent cores from the 2011 coring program.
- Dam survey information, including the recent survey using photogrammetric techniques (2011).
- Geotechnical data of the site provided by AEL&P.

Task 2: Seismic analysis ground motions development

- Detailed review of the most recent seismic hazard analysis.
- Update of seismic hazard analysis for the dam site, including probabilistic and deterministic seismic hazard analysis.
- Development of three sets of ground motions for the dynamic time history analysis, each including two horizontal components (upstream-downstream and cross-canyon directions) and one vertical component.
- Preparation of a technical memorandum regarding input for the seismic evaluation report (Task 3 below) documenting the seismic hazard analysis and ground motion development.

Task 3: Three-dimensional nonlinear finite element analysis

- Selection of material properties for the dam concrete and foundation rock, and properties for the concrete/foundation rock and contraction joint contact.
- Development of a three-dimensional finite element model using ANSYS Version 14.0.
- Performing a nonlinear static finite element analysis of the dam, including thermal loading, to establish a baseline state of stress in the dam to be used as the initial condition for the seismic analysis.

- Performing a nonlinear dynamic finite element analysis of the dam, using the three sets of ground motions developed in Task 2 (above) to determine acceptable reservoir operating levels.

1.4 Report Qualifications and Limitations

The findings of this report are based on the readily available data and information obtained from public and private sources, and provided by AEL&P. MWH has relied upon the information and data without independent verification, except only to the extent such verification was expressly included in the Services. MWH’s opinions, recommendations and assessments are limited by a) the accuracy and completeness of information upon which it has reasonably relied, b) schedule constraints or scope limitations, c) unknown or variable site or other conditions, d) other factors beyond MWH’s control. Additional studies (at greater cost) may or may not disclose information which may significantly modify the findings of this report. In the event that there are any changes in the nature of available data and/or historical documents of the dam, the conclusions and recommendations contained in the report will need to be reevaluated by MWH in light of the proposed changes or additional information obtained.

This report does not reflect or incorporate information relative to any latent defects not apparent from the data upon which the report is based, as identified in Section 2.0 and throughout the report.

This report was prepared solely for the benefit of AEL&P. No other entity or person shall use or rely upon this report or any of MWH's work products unless expressly authorized by MWH. Any use of or reliance upon MWH's work product by any party, other than AEL&P, shall be solely at the risk of such party.

1.5 Evaluation Team

The following individuals were the key personnel involved in the preparation of this report:

- Scott Willis, AEL&P Vice President, Generation
- David P. Thompson, P.E., MWH Project Manager
- Glenn S. Tarbox, P.E., MWH Senior Technical Advisor
- Vik Iso-Ahola, P.E., MWH Principal Analysis Engineer
- Jennifer Jones, MWH Associate Structural Engineer

1.6 Professional Certification

This report has been prepared by MWH Americas, Inc (MWH) under the professional supervision of the Principal and senior staff whose seals and signatures appear herein. The findings, interpretations of data, recommendations, specifications, or professional opinions are presented within the limits prescribed by available information at the time the report was prepared, in accordance with generally accepted professional engineering practice and within the requirements by Alaska Electric Light and Power Company. There is no other warranty, either expressed or implied.

STATE OF ALASKA
49TH
DAVID P. THOMPSON
No. 9317
REGISTERED PROFESSIONAL ENGINEER

STATE OF ALASKA
49TH
Glenn S. Tarbox
No. CE 4871
REGISTERED PROFESSIONAL ENGINEER

David P. Thompson, P.E.
Vice President and Project Manager
Principal Civil Engineer

Glenn S. Tarbox, P.E., F. ASCE, SECB
Senior Vice President, Technical Advisor
Global Dams Practice Leader

1.7 Copyright

2.0 REVIEW OF TECHNICAL DATA

The following documents were provided by AEL&P for MWH review:

- Alaska Gastineau Mining Company, Salmon Creek Power Project, October 1913 Construction Drawings, Plates 1-6.
- Alaska Gastineau Mining Company, Salmon Creek Application for Final Power Permit, August 1917 As-Built Construction Drawings, Exhibits A1 and A2.
- Historical concrete testing correspondence provided by AEL&P, miscellaneous dates and personnel involved.
- Historical construction reports and correspondence provided by AEL&P, miscellaneous dates and personnel involved.
- Historical construction photographs provided by AEL&P, miscellaneous dates.
- A.J. Industries, Inc., Repair of Salmon Creek Dam, February 1962 As-Built Drawings, Exhibits K and L.
- A.J. Industries, Inc., Revision of Repairs of Salmon Creek Dam, July 1968 As-Built Drawings, Exhibit L.
- James M. Montgomery Consulting Engineers, Inc. (La Jolla, CA), Salmon Creek Dam Core Drilling, June 1978 Core Drilling Schematic.
- Historical correspondence (1978) provided by AEL&P, between the following entities: James M. Montgomery Consulting Engineers, Inc., Lewis H. Tuthill (Concrete Engineering Consultant), Alfred L. Parme (Consulting Engineer), and AEL&P.
- Converse Consultants (Seattle, WA), "Seismic Evaluation of Salmon Creek Dam," 14 September 1982.
- James M. Montgomery Consulting Engineers, Inc. (La Jolla, CA), "Report on Safety Inspection Salmon Creek Dam FERC Project No. 2307-Alaska," February 1983.
- James M. Montgomery Consulting Engineers, Inc. (La Jolla, CA), "Supplemental Report on Safety Inspection Salmon Creek Dam FERC Project No. 2307-Alaska," March 1983.
- MWH (Bellevue, WA), "Salmon Creek Hydroelectric Project, Part 12 Sam Safety and Inspection Report," December 2002.
- MWH (Bellevue, WA), "Supporting Technical Information, Salmon Creek Hydroelectric Project, FERC Project No. 2307," November 2007.
- Mullikin Surveys, Salmon Creek Dam Point Cloud Cross Sections and Data, April 2011 Survey.

- Krazan and Associates (Bothell, WA), "Salmon Creek Dam, AK Laboratory Testing of Concrete Core Samples," 20 October 2011.

3.0 SEISMIC HAZARD ANALYSIS

A review and revision of previous seismic hazard analyses was performed as part of this dam stability evaluation. The updated seismic hazard assessment (SHA) performed for the project site, performed in general accordance with FERC engineering guidelines (Idriss, 2007), evaluated regional geologic setting, characterized seismic sources, provided recommendations for the maximum credible earthquake and included recommended earthquake time histories for the FEM analyses of the dam. Three earthquake time histories were selected based on their source characteristics and scaled or modified to match the selected site response spectrum. The earthquake motions were modified by simple scaling (i.e., a single factor applied to the entire motion) or spectral matching, compare well to the site response curve and controlling ground motion, and were not otherwise modified (i.e., number of cycles, Aria's intensity, and predominate frequency). The results from the SHA reduced the anticipated peak ground acceleration from 0.35g in the previous analysis (JMM, 1983) to 0.18g, and from a magnitude 8.0 earthquake at 34 km to a magnitude 7.3 at 53 km.

MWH's seismic hazard analysis report is included in **Appendix A**.

4.0 MATERIAL PROPERTIES EVALUATION

A thorough review of the reference documents provided was performed to assess the current condition of the dam. The review materials included historical construction information, material properties developed from three coring programs, and overall observations of the latest concrete condition. Statistical analyses were performed on the concrete testing results and engineering judgment was applied to establish the material properties and threshold values for the dam concrete and foundation materials. The established properties were used for the three-dimensional linear and non-linear finite element method (3D FEM) structural analyses of Salmon Creek Dam.

4.1 Investigation of Dam Properties

4.1.1 Analysis of Material Properties from Coring Programs

Three separate concrete coring programs were performed in 1967, 1982, and 2011 at Salmon Creek Dam in order to investigate the ongoing weathering and freeze-thaw deterioration of the concrete. Most of the cores in 1967 were taken vertically from the crest of the dam, and included testing of the concrete samples taken at various depths of the core holes. A few cores were taken horizontally on the downstream face of the dam. Samples were tested for compressive strength and modulus of elasticity. The coring was performed using a NX-size coring bit (2.06 inch diameter); as a result, the compressive strength test results were adjusted by a factor of approximately 0.76 to account for the difference in the sample size (values under "Adjusted Compressive Strength" in **Table 1**). It should be noted that the modulus of elasticity was not directly measured; rather, this value was estimated for each sample using previously published correlations to compressive strength. Also, two of the horizontal cores (near the left abutment of the dam) went all the way through the dam with no recovery of solid concrete samples (1967 sampling program).

In 1982, select NX core samples remaining from the 1967 coring program were tested for compressive strength, splitting tensile strength, modulus of elasticity, and Poisson's ratio. The tests were performed by Testing Engineers, Inc. and provided to International Engineering, Inc. (IECO) as part of their seismic stability evaluation of the dam. A drawing with material properties from the 1967 and 1982 coring programs is shown in **Figure 2**, as well as in tabular format in **Table 1** below (JMM, 1983).

Table 1. Summary of Concrete Properties from 1967 & 1982 Testing Programs

Core Hole	*Elevation (ft)*	*Adjusted Compressive Strength (psi)*	*Modulus of Elasticity, E (10^6 psi)*
5V	1167	2490	2.7
	1154	3500	3.1
	1143	4800	3.6
	1133	4860	3.8
	1129	4410	3.4
2V	1169	2010	2.4
	1158	1430	2.0
	1148	4750	3.8
	1139	4640	3.6
	1129	4180	3.2
	1119	2150	2.4
	1109	4180	3.5
	1100	3500	3.0
	1088	4300	4.0
	1077	7450	4.2
	1073	6480*	4.3
	1067	5200	3.6
	1057	3870	3.4
	1049	3180	3.1
	1043	3060	2.7
1V	1170	5420	5.2
	1162	5630*	5.0
	1159	4960	4.6
	1151	5420	4.6
	1138	3380	3.1
	1131	6020*	4.1
	1129	3050	3.0
	1119	5200	4.1
	1107	2260	2.3
	1104	5170*	3.5
	1100	3500	2.9
	1089	3610	3.1
	1080	5530	4.2
	1071	4070	3.1
	1058	3390	3.1
	1048	3960	3.3
	1036	3620	3.2
	1028	2940	2.8
3V	1172	3630	3.0
	1168	7390*	4.1

Core Hole	*Elevation (ft)*	*Adjusted Compressive Strength (psi)*	*Modulus of Elasticity, E (10^6 psi)*
3V	1165	4800	3.4
	1151	5030	3.4
	1142	4020	3.0
	1132	4580	4.1
	1122	900	1.7
	1115	5530*	4.4
	1112	4700	4.1
	1102	4800	4.0
	1092	4240	4.0
	1082	3360	3.2
	1072	3390	3.1
	1061	4750	3.9
	1054	4520	3.5
	1043	3050	2.9
	1031	2830	2.8
4V	1167	2190	2.6
	1147	6300*	3.2
	1145	4410	2.7
	1142	4410	2.8
	1135	4980	3.5
	1132	6570*	4.0
	1124	3730	3.1
10H	1121	2720	2.9
9H	1128	2830	3.0
8H	1051	3910	3.3
8H	1049	2260	2.4
7H	1095	3170	2.6
6H	1138	4910	3.1
5H	1117	4420	3.8
4H	1148	3390	3.0
3H	1134	5280	4.4
3H	1131	3500	3.4

Core Hole	*Elevation (ft)*	*Splitting Tensile Strength (psi)*
1V	1162	895
2V	1073	625
3V	1121	665
4V	1133	743
4H	1166	659
8H	1166	449

* samples were tested in 1982 (all others tested in 1967). *V = vertical core, H = horizontal core.*

During MWH's 2011 coring program, a total of 39 cores were taken horizontally from the dam, 23 from the downstream face of the dam, and 16 from the upstream face of the dam. In most locations, suitable samples of concrete (i.e., without cracks or fractures) were not reached for one- to two-feet into the dam, and, in general, samples suitable for testing in targeted areas were not always obtained. In a number of the core holes, the first few feet of concrete was cored with no solid concrete sample recovery (i.e., the concrete completely deteriorated upon drilling). The maximum coring and sampling depth was 40 inches, and a majority of coreholes were advanced to about 24-36 inches. Laboratory testing of the cores was performed by Krazan and Associates (see **Appendix B**). Test results are summarized in **Table 2** below, where the listed Core IDs are depicted in **Figures 3 & 4**.

Table 2. Summary of Concrete Properties from 2011 Testing Program

Downstream Face Cores

Core ID	Elevation (ft)	Compressive Strength (psi)	Splitting Tensile Strength (psi)	Modulus of Elasticity (10^6 psi)	Poisson's Ratio
D211	1135	3170			
D221	1125		290		
D241	1065	1180			
D252	1038		415		
D431	1111	3360			
D441	1067		780		
D451	1040	3600			
D511	1135	4020			
D521	1125	5210*		3.30	0.148
D531	1105		445		
D541	1077		385		
D611	1145	4960*		2.45	0.178
D612	1135	2370			
D621	1115		495		

Upstream Face Cores

Core ID	Elevation (ft)	Compressive Strength (psi)	Splitting Tensile Strength (psi)	Modulus of Elasticity (10^6 psi)	Poisson's Ratio
U121	1123	3200			
U111	1145		695		
U221	1125	1740	380		
U241	1058		435		
U421	1128	5010*		3.15	0.161
U441	1057	3410			
U511	1147		400		
U521	1127	1190			
U531	1105		355		
U541	1057	2730			
U611	1148				
U621	1129	4700			

* The compressive strength values determined from modulus tests were not further considered in the determination of material properties in this analysis, due to difference in testing procedure (ASTM C39 vs. ASTM C469).

The test results from the 1967, 1982, and 2011 coring programs were compared in order to determine whether any correlation exists between the sets of data, and between concrete properties (i.e., compressive strength and modulus of elasticity) and elevation. These comparisons are shown in **Figures 5 & 6.** Similarly, in **Figure 7**, the elevation versus splitting tensile strength data from the 2011 coring program were plotted.

Figure 8 compiles the material properties of the three coring programs on the face of the dam. Comparing subsets of the results in similar regions on the dam face suggests that cores do not show any clear trends in concrete properties (e.g., no clear difference in strength between concrete near the right and left abutments). The data from the plots above are further analyzed and tested for trends using statistical methods in the following sections.

4.1.2 Evaluation of Contraction Joints

Due to a general lack of historical construction information of Salmon Creek Dam, it is unclear whether or not contraction joints were incorporated during the construction of the dam. However, of note is the series of letters between Mr. F. G. Baum (F. G. Baum & Company, Inc., designers of Salmon Creek Dam) and Mr. H. L. Wollenberg (Chief Engineer, Alaska Gastineau Mining Co.) that recommends the installation of contraction joints into the dam after a portion of the concrete had already been poured. These notes are found in **Appendix C**. The following notes are of particular interest:

- In the first letter of the series (page 2, **Appendix C**), by Lars Jorgenson (F. G. Baum & Company, Inc., pioneer of the constant angle arch dam), he quotes, "While this is probably not entirely necessary as I do not think the dam will crack, it will do no harm to put in two contraction joints, one on each side of the canyon, beginning at the ground at about the elevation of the present stage of the dam, that is, about 72 feet above the base." This indicates that the dam was at a minimum elevation of 1,082 feet when contraction joints were implemented.

- Further correspondence later indicated that it would be ideal to place contraction joints at thirds along the dam. This is seen in a letter from Chief Engineer H. L. Wollenberg, on May 14, 1914 (page 9, **Appendix C**), who writes, "We are carrying up two expansion joints located at about the 1/3 points of the dam." In comparison to a photo in August 1914 (**Figure 9**), it appears that the contraction joints were most likely started below El. 1082. The distance between the ground and the current maximum lift height in the photo seems lower than the previously described elevation of 1,082 feet would suggest.

Construction photos (see **Figure 9**) suggest that the dam was placed in blocks with at least two vertical construction or contraction joints. The historical construction photos were taken from one location; thus, it was impossible to establish whether or not there were more joints at locations nearer the opposing abutment. Also, construction drawings do not indicate any contraction joints. Using the recommendations provided in the May 1914 letter and progress of construction at the time of the letter, it was assumed that two joints were started at the foundation at about El. 1050 near the third points (length measured along the dam crest) and continued vertically to the top of the dam.

4.2 Statistical Analysis Methods

To evaluate the effects of age on the compressive strength and splitting tensile strength of the concrete, a series of statistical analyses were performed to compare the 1967, 1982, and 2011 data. Statistical tests could not be performed for the modulus of elasticity (E) and Poisson's ratio (ν) due to the small data set size that was produced only during the 2011 testing program (as mentioned previously, the 1967 testing program did not directly measure E and ν). Overall, the statistical evaluation was performed to provide a rational method in evaluating the laboratory testing data, which subsequently used to establish the material properties input into the structural analysis model.

The statistical analysis methods used to compare these data over time were selected to compare and validate (i.e., accept or reject a null hypothesis about comparisons between data sets) whether trends exist in the data over time. For example, when the statistical tests show a difference in population mean between discrete sets of data taken at two different points in time, it can be inferred that an increasing or decreasing trend in the data exists over time. A summary of each method used is provided below:

- The "f-Test" method was first performed to evaluate the variances of two sample sets of data. If the "F" test statistic falls outside of two bounds, $F < F_{1-\alpha/2,v1,v2}$ and $F > F_{\alpha/2,v1,v2}$, (where α=5% and v_1 and v_2 are the sample sizes) then the null hypothesis (that the variances are equal) is rejected, and it is concluded that the variances of the two data sets are not equal.

- The primary method to evaluate the data set was the single factor analysis of variance (ANOVA) method, which hypothesizes and tests whether the population means of sample sets of data are equal. If they are different, then the resultant "F" statistic will be higher than the critical F value (F_{crit}), and the "p" value will be less than 5% (assuming α=5% significance level).

- In the "t-Test" method, if the "t" statistic is greater than "t-critical", then the null hypothesis (that the population means are equal) is rejected and it is inferred that the population means of the two data sets differ and thus show a possible trend.

4.3 Statistical Analysis Results

The results of the statistical analysis tests are summarized below for each material property vs. age. Detailed tabular results from the analyses are provided in **Appendix D**.

4.3.1 Difference in Variances (f-Test)

Two compressive strength data sets were considered in the f-Test to determine if the variance is equal between each set – the first data set includes all data from the 1967 coring program (both those tested in 1967, and those later tested in 1982), and the second data set includes all data from the 2011 coring program. The f-Test found a test statistic of 1.408, which fell out of the bound $F < F_{1-\alpha/2,v1,v2}$ (equal to 2.199), indicating that the variances of the two sample sets are not equal.

4.3.2 Comparison of Compressive Strength vs. Age of Concrete

An ANOVA test was performed with compressive strength data from 1967, 1982, and 2011. The results of the test showed a difference in the means between all groups, with an F value of 21.74, which is greater than the F_{crit} of 3.11, and a P-value of 0.00000003, which is less than 5%. These results were confirmed by the t-Test performed on these same sets of data. Three t-Tests were performed, comparing data from 1967 to 2011, data from both 1967 and 1982 to 2011, and data from 1967 to 1982, and all yielding results of t_{stat} greater than t_{crit}. The test results showed that there was an *increase* in average compressive strength from 1967 to 1982, and then a decrease in average compressive strength from both 1982 to 2011 and 1967 to 2011.

4.3.3 Comparison of Compressive Strength at Discrete Elevation Ranges

Elevation 1110-1150

Two ANOVA tests were performed for the elevation range between 1110-1150 feet. One test included data from all three coring programs, while the other test only included data from 1967 and 2011. Both of these ANOVA tests found F values greater than F_{crit}, and P-values well below 5%, indicating a difference in the means between the groups. The t-Test for this elevation range also confirmed a difference in the means between the data groups, finding t_{stat} to be greater than t_{crit}, suggesting that the average compressive strength value in this elevation range had dropped from 1967 to 2011.

Below Elevation 1075

The compressive strength data from 1967 and 2011 was compared in the ANOVA test for this elevation range. The results indicated that below El. 1075, the sample means do *not* vary, unlike elsewhere on the dam. In this ANOVA test, an F value of 3.44 was less than an F_{crit} of 4.38, while the p-value of 7.9% was greater than 5%. These results were also compared to a t-Test, which found that the t_{stat} was less than the t_{crit}, indicating that the average compressive strength value at elevations below 1075 had not changed from 1967 to 2011. It should be noted that a data set of only four values from 2011 was used to perform this test, which is less than the typically suggested sample set of 10 or greater.

4.3.4 Compressive Strength Comparison between Discrete Elevation Ranges

Two ANOVA tests were performed that compared the compressive strength data set between El. 1110-1150 to the data set below El. 1075. The first test included data from all testing programs (1967, 1982, and 2011), while the second test only compared data from the 1967 testing program. Both tests found F values that were smaller than F_{crit} and P-values much greater than 5%, indicating that the difference in the means does not vary; thus, indicating no difference in compressive strength between upper and lower elevations of the dam.

4.3.5 Comparison of Splitting Tensile Strength vs. Age of Concrete

An ANOVA test was performed with splitting tensile strength data from 1982 and 2011. The results of the test showed a difference in the means between all groups, with an F value of 8.02, which is greater than the F_{crit} of 4.54, and a P-value of 0.012, which is less than 5%. The t-Test that was also performed on these same sets of data confirmed the results of the ANOVA test. The t-Test found that the t_{stat} was greater than t_{crit}, indicating that the sample means do vary. The data set from 1982 included only six values, which is less than the suggested sample set of 10 or greater, but was utilized since it was the only splitting tensile strength data available. These results indicated an overall decrease in average splitting tensile strength from 1982 to 2011.

4.4 Statistical Analysis Findings

The tests in Section 4.3 were performed to evaluate whether possible trends over time or elevation exist for the compressive and splitting tensile strength of Salmon Creek Dam. Some possible trends were identified; however, it should be noted these statistical analyses were performed assuming that all the concrete test data could be treated equally, where no other factors were assumed to influence the data other than time or elevation. In fact, the analyses were performed across data sets from concrete cores taken at different times using different sized core samples (2” in 1967 and 1982 vs. 6” in 2011), and were tested using inconsistent preparation and test methods. The differences between the testing programs are summarized below:

- The core samples tested in 1982 were actually cores taken during the 1967 program. There is no record in the 1983 International Engineering Company, Inc. (IECO) report attached to the 1983 Part 12 Inspection Report (JMM, 1983) as to how these samples were stored over the fifteen year period after sampling, or if any portion of the testing procedure was different in 1982 versus when the cores were taken in 1967. Overall, the mean compressive strength of 1982 tests is much higher than those in 1967, which is suspect, since the samples were taken at the same time, at similar locations, and were tested on concrete that was not expected to notably gain strength due to its 50+ year age. The IECO report does not discuss or evaluate the substantial increase in strength, nor explain why the overall average of 1967 and 1982 data was used in place of updated tests that showed an adjusted average compressive strength of 5900 psi and average modulus of elasticity of 4,000,000 psi.

- The 1967 cores were 2.06" in diameter, which likely misleadingly increased compressive strength results, and possibly splitting tensile strength results obtained during tests performed in 1982, due to the 3" nominal maximum coarse aggregate size within the concrete. Core samples with coarse aggregate spanning the entire diameter of the core will influence the strength behavior of the sample due to the higher strength large aggregate, which can be stronger than the composite concrete matrix. Although the 1982 Testing Engineers, Inc. testing report in the attachments to the 1983 Part 12 Inspection Report (JMM, 1983) shows core sample aggregate size of 0.75" to 1" and subsequently IECO reports a reduction factor was applied to the 1967 and 1982 results to account for the small core size, it is possible that the 1967 (and therefore, 1982) cores are stronger than those taken in 2011 only due to the difference in core sample size. The current ASTM C42, Standard Test Method for Obtaining and Testing Drilled Cores and Sawed Beams of Concrete, requires that concrete core specimens have a diameter of at least than 2 times the nominal maximum aggregate size.

- The depth of concrete sampling in 2011 was between 2- and 3-feet, which is generally within the estimated range of depth of freeze-thaw damage and deterioration on the dam faces. As a result, the 2011 weaker outer layer of concrete is being compared to the 1967 vertical coring data that has a substantial sample set from well within the interior of the dam.

- Many locations cored in 2011 yielded no intact concrete to test. This may have been the case in 1967 as well, but locations that were sampled but fractured were not reported. Areas with fractured, untestable concrete indicate a weaker overall strength. The low strength of untestable concrete is not captured in the averages of the core sample test data sets, but should be considered when determining the composite strength of the dam.

Based on the inconsistencies between the test data sets, the suspect 1982 test results, and the exclusion of untestable samples in averages, the conclusions that are presented in the following subsections use engineering judgment to assess the validity of the trends (if any) indicated by the statistical tests. In other words, the presented statistical evaluations were used as a "first pass" rational method to test for possible trends in the material properties data against which engineering judgment could be used, rather than applying initial engineering judgments and relating those judgments to visual observations of possible trends in the data.

4.4.1 Comparison of Compressive Strength vs. Age of Concrete

The statistical tests showed that there is a difference in population means for concrete compressive strength versus age, between all three coring programs. The difference between these data sets, however, may be due to other conditions, as previously mentioned. These include, but are not limited to, difference in core size, sample storage between 1967 and 1982, sample preparation and testing methods used in 1967 and 1982, and grouting repair work in 1967.

Of particular note is the *increase* in average compressive strength of over 2,200 psi from 1967 to 1982, which might be expected of concrete in early hardening stages, but not 50+ year old concrete. It is possible that a combination of error in sampling, preparation, storage, and testing methods contributed to the increase from 1967 to 1982. When 1982 data is excluded, the comparison of averages between 1967 and 2011 shows a decrease over this 43 year period by about 1,200 psi. This trend may suggest that the concrete strength has declined over time; however, it should be considered that strengths may not be directly correlated due to the different core sizes and the type of concrete encountered (freeze-thaw damaged concrete at surface vs. interior mass concrete).

4.4.2 Comparison of Compressive Strength at Discrete Elevation Ranges

The statistical tests indicated a difference in population means for compressive strength between elevations 1110-1150 feet, demonstrating that concrete in upper regions of the dam may have declined in strength over time. Below elevation 1075 feet, the statistical tests showed no difference in the population means for compressive strength, indicating that concrete strength in the thicker, lower regions of the dam has not changed over time (noting, however, that the 2011 data set had only 4 values). Similar to the tests in Section 4.4.1 above, it should be considered that strengths may not be directly correlated due to the different core sizes and the type of concrete encountered (i.e., freeze-thaw damaged concrete at surface vs. interior mass concrete).

4.4.3 Compressive Strength Comparison Between Discrete Elevation Ranges

Two statistical tests were performed to determine if there was any difference between the compressive strength at elevation ranges El. 1110-1150 and below El. 1075. The first test considered data from all testing programs, while the second test compared only data from the 1967 coring program. Both of these tests showed no difference in population means for the compressive strength between El. 1110-1150 and below El. 1075, indicating that there is no difference in concrete deterioration across different regions of the dam.

4.4.4 Comparison of Splitting Tensile Strength vs. Age of Concrete

The statistical tests showed that there is a difference in population means for concrete splitting tensile strength versus age, between the 1982 and 2011 tests. It should be noted that the 1982 splitting tensile tests were, again, performed on 1967 cores, that may have been sampled, stored, and prepared for testing using different methods than what was performed in 2011. No splitting tensile strength tests were performed in 1967, so no correlation from the 1982 tests can be drawn to their original cores. However, similar to the compressive strength of the concrete, there is indication that the splitting tensile strength of the dam has decreased over time.

4.5 Evaluation of 1967 and 1982 Core Testing Data

Following the statistical tests in Section 4.4.1, which indicated a substantial increase in compressive strength from 1967 to 1982, the modulus of elasticity was computed using the tested compressive strengths to further evaluate differences between data sets and at specific regions of the dam. **Table 3** highlights the increase from 1967 to 1982 in average compressive strength and modulus of elasticity by elevation above and below El. 1140. **Table 3** also shows that the modulus values used in the 1982 FEM analysis (JMM, 1983) were lower than the tested averages at comparable elevations. Furthermore, the modulus values shown in **Table 4** at the center and the "wings" (i.e., right and left sides of arch above El. 1140) of the dam are greater than the modulus values used in the 1982 FEM analysis. It should be noted that the results in **Table 4** are based on four core tests that were sampled from a single vertical core hole at the center of the dam, which provides for a very small sample set that may not provide an accurate representation of strength in this region of the dam.

Table 3. 1967 and 1982 Computed Modulus of Elasticity

		Average Compressive Strength (psi)	Calculated Modulus of Elasticity, E* ($x10^{-6}$ psi)	Modulus of Elasticity, E used 1982 FEM model ($x10^{-6}$ psi)
1967	*Above El. 1140*	3921	3.57	2.60 to 3.80
1967	*Below El. 1140*	3879	3.55	3.00
1982	*Above El. 1140*	6440	4.57	2.60 to 3.80
1982	*Below El. 1140*	5954	4.40	3.00

* calculated based on ACI 318-05, 8.5.1 formula, $E = 57{,}000(f'_c)^{1/2}$

Table 4. 1967 and 1982 Computed Modulus of Elasticity at FEM Zones

		Average Compressive Strength (psi)	Calculated Modulus of Elasticity, E* ($x10^{-6}$ psi)	Modulus of Elasticity, E used 1982 FEM model ($x10^{-6}$ psi)
Center	*Above El. 1140*	5358	4.17	3.80
Wings	*Above El. 1140*	4491	3.82	2.60

- includes tests from both 1967 and 1982, due to small data set.

* calculated based on ACI 318-05, 8.5.1 formula, $E = 57{,}000(f'_c)^{1/2}$

A comparison of the data against observations and visual documentation indicates that the ongoing deterioration of the concrete at the dam faces near the top center portion of the dam is not notably different to justify such a substantial increase (46%) in modulus from the “wings” to the center of the dam. When considering photos from the 1967 repairs (see **Figure 10**), it is clear that heavy deterioration had occurred across most of the dam face, including the central portion of the arch in 1967. Similarly, **Figure 11** shows a rendering of the downstream face of the dam that shows even distribution of deterioration damage. Also, recent 2011 cores above El. 1140 near the central portion of the arch were not all intact; many were fractured and could not be used for strength testing, as seen in **Figure 8**.

4.6 Evaluation of 2011 Core Testing Data

The core test data from the 2011 investigation were separated into regions on the dam face to further assess data trends. Since only three samples from the 2011 coring program were tested for the modulus of elasticity (E) and for Poisson’s ratio (ν), statistical tests for trends were not performed. Similarly, density and bulk specific gravity were tested in four cores and, thus, were only averaged. These results are shown in **Table 5**.

Table 5. Tested Material Properties, 2011 Coring Program

Location	Modulus of Elasticity, E (psi)	Poisson's Ratio, ν
Center of dam, El. 1125	3,300,000	0.148
Near Left Abutment, El. 1145	2,450,000	0.178
Center of dam, El. 1125	3,150,000	0.161
Average	2,970,000	0.162

Location	Bulk Specific Gravity, Dry	Density (lb/ft^3)
D121	2.529	157.9
D421	2.458	153.5
U441	2.443	152.5
U611	2.548	159.1
Average	2.495	155.7

Given the limited number of modulus of elasticity tests performed, compressive strengths from the overall testing program were converted to modulus of elasticity using a published American Concrete Institute (ACI) formula that correlates compressive strength to modulus of elasticity (ACI, 2005). The computed values are summarized in **Table 6**. As shown, the average of the computed modulus of elasticity closely matches the average of the tested modulus values.

Table 6. 2011 Computed Modulus of Elasticity

Elevation (ft)	Compressive Strength (psi)	Calculated Modulus of Elasticity, E* (x10^{-6} psi)	Elevation (ft)	Tested Modulus of Elasticity, E* (x10^{-6} psi)
			1,145	2.45
1,135	3,170	3.21		
1,135	4,020	3.61		
1,135	2,370	2.77		
1,129	4,700	3.91	1,128	3.15
1,127	1,190	1.97		
1,125	1,740	2.38	1,125	3.30
1,123	3,200	3.22		
1,111	3,360	3.30		
1,065	1,180	1.96		
1,057	3,410	3.33		
1,057	2,730	2.98		
1,040	3,600	3.42		
Average	2,889	3.01	Average	2.97

* calculated based on ACI formula 318-05, 8.5.1, $E = 57{,}000(f'_c)^{1/2}$

4.7 Statistical Analysis Conclusions

The tests from the statistical analysis showed that average compressive strength increased from 1967 to 1982, then decreased when tested in 2011, and, when evaluated in isolated elevation ranges, showed a similar decline in average over time in the upper portion of the arch (El. 1110 to 1150 feet). Similarly, the statistical analysis tests indicated that the average splitting tensile strength decreased from 1982 to 2011. Although this evaluation showed changing trends in average strength over time, it was found that the differences between data sets could have been influenced by other factors, such as difference in core sample size, sample preparation and handling, depth of core samples, and core holes that had untestable (weak) concrete.

Unresolved differences between the average test results from 1982 and the values selected for the 1982 FEM analysis highlight the need for consideration of other factors. In addition, the evaluation of properties in regions of the dam (i.e., elevation ranges and areas of elevations divided into central, left and right zones) showed no clear trends to provide a basis for varying material properties in the dam. As such, the structural analyses presented in this report consider material properties from the entire concrete testing data set from 1967 through 2011. The selected material properties are discussed in the following section.

4.8 Material Properties Used in the Model

The results of the statistical and qualitative evaluation of the 1967, 1982, and 2011 concrete strength testing data were used to select a limited set of scenarios to evaluate the sensitivity of the dam response under earthquake loading. First, the previously established finite element model material properties from the 1982 analysis were compared against the comparison of the concrete testing results from 1967, 1982 and 2011. Included in **Table 7** is the finite element mesh that was used in the 1982 analysis, showing the previously selected zones of modulus of elasticity in the dam; see **Appendix E** for a larger view of this schematic.

Table 7. Analysis Material Properties, 1982 Part 12 Inspection Report

	Modulus of Elasticity (x10^6 psi)			
	1982 FEM Properties	1967 Cores, Calculated E	1982 Cores, Calculated E	2011 Core Data
Concrete, below EL 1135	3.00	3.30	4.06	Average: 2.97
Concrete, center above EL 1135	3.80	4.38	5.00	
Concrete, wings above EL 1135	2.60	3.01	3.65	Left Abut: 2.45
Foundation, bottom of dam	3.00			
Foundation, Right Abutment	2.00			
Foundation, Left Abutment	1.75			

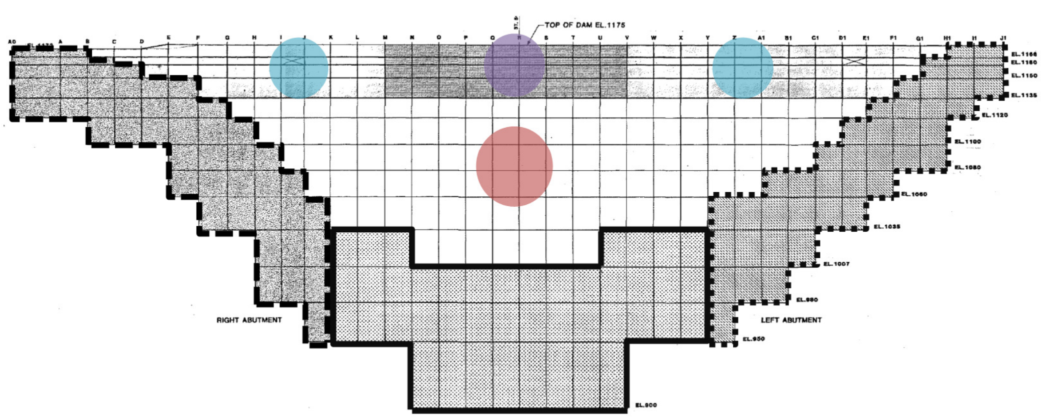

The comparison above demonstrates that in 2011, other than a single tested value at El. 1145 near the left abutment (2,450,000 psi), the variation in the modulus of elasticity data (tested and computed) do not show any clear trends that would support using a significantly lower (or higher) modulus of elasticity at higher elevations in the dam (**Table 7**). As such, the primary concrete material properties selected for the finite element analysis are based on the averages from the 2011 cores presented in **Table 8**. Also, since no new geotechnical investigation has been performed, material properties for the foundation rock from the 1982 analysis were used (**Table 8**).

Table 8. Material Properties for Analysis, 2012 Seismic Evaluation

		Foundation Rock		
	Dam	**Center**: below center of CJs, vertically from El. 1050 to bottom	**Right Abutment**: from right CJ to outside of foundation	**Left Abutment**: from left CJ to outside of foundation
Modulus of Elasticity, E (psi)	2,970,000	3,000,000	2,000,000	1,750,000
Poisson's Ratio, v	0.162	0.2	0.2	0.2
Density (pcf)	155.7	154	154	154

Note: CJ means contraction joint

In consideration of the variability of the concrete test data and, further, in order to evaluate the sensitivity of the dam response, an additional model scenario similar to the 1982 FEM analysis was developed, creating transition zones of varied material properties at elevations and zones within the dam. These properties are shown in **Table 9**. The modulus of elasticity in the main bottom portion of the dam (shown in two colors of grey) and on the top sides of the dam near the abutments (shown in yellow) were taken from data available in those vicinities, as seen in **Table 9**. To avoid sharp transitions of material properties, two transition zones were created between these areas with intermediate modulus values. These areas of transition reduce high concentrations of stress that are simply caused by abrupt changes modulus of elasticity between adjacent elements in the FEM model. These transition zones were simulated to more accurately represent in-situ conditions within the dam concrete, where sharp transitions in concrete strength have not been demonstrated to exist. Poisson's ratio and the density were the same as the values used in the primary FEM analyses.

Table 9. Varied Material Properties (Compare to 1982 Part 12 Inspection FEA)

	Color in Model	Modulus of Elasticity, E (psi)	Poisson's Ratio, ν	Density (pcf)
Center between Contraction Joints		2,970,000	0.162	155.7
Sides of Contraction Joints Near Abutments		2,970,000	0.162	155.7
First Transition Zone		2,850,000	0.162	155.7
Second Transition Zone		2,650,000	0.162	155.7
Top Sides Near Abutments		2,450,000	0.162	155.7

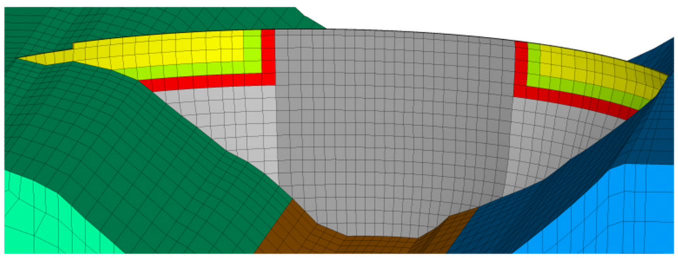

4.9 Tensile and Compressive Strength Threshold Capacities

Tested material properties from the three coring programs (1967, 1982 and 2011) were compared to determine the dynamic material properties of Salmon Creek Dam. The average strengths from each program are shown in **Table 10**. As discussed in Section 4.7, there is no consistency in testing methodology, nor any trends between the three testing programs, so the structural analyses in this report largely consider the strengths determined from the 2011 coring program, but include evaluation of the range of strength data from all the coring programs.

In **Table 10**, the static compressive strength and splitting tensile strengths are tested material properties. Using standard practice developed by USBR, the static compressive strength and the splitting tensile strength were converted to dynamic strengths (USBR, 2006). Splitting tensile strength is first halved to find the direct tensile strength, which is then multiplied by a factor of 1.5 to determine the dynamic tensile strength. Likewise, the static compressive strength is also multiplied by a factor of 1.5 to find its corresponding dynamic strength. These correlation formulas are shown in **Table 10**, where the final dynamic strength values used in this analysis are shown in bold.

Table 10. Average Dynamic Tensile and Compressive Strength Capacities

Testing Program	Static Compressive Strength (psi) f'_c	Dynamic Compressive Strength (psi) $f'_{dc} = 1.5(f'_c)$	Splitting Tensile Strength (psi) f_{st}	Direct Tensile Strength (psi) $f_{dt} = 0.5(f_{st})$	Dynamic Tensile Strength (psi) $f_{dst} = 1.5(f_{dt})$
1967	3940	5910	--	--	--
1982	6136	9204	673	336	505
2011	2889	**4334**	461	231	**346**

5.0 STRUCTURAL STABILITY ANALYSIS

MWH's approach to the structural stability evaluation of Salmon Creek Dam is described below. In general, the methodology used to evaluate the arch dam was in conformance with the procedures outlined in Chapter 11 of FERC's Engineering Guidelines for Evaluation of Hydropower Projects (FERC, 1999).

5.1 Existing Dam Geometry

Salmon Creek Dam has experienced significant concrete deterioration from freeze-thaw cycles since construction. A rehabilitation program was implemented in 1967 to repair failing portions of the dam. Across most of the upper portion of the dam face, deteriorating concrete was chipped off of the surface of the dam, including depths of several feet at some locations, and thereafter, a fresh layer of gunite (shotcrete) was applied to fill the chipped areas and provide a new concrete surface on the dam faces. Photos of the rehabilitation are shown in **Figure 10**. It was noted that the amount of seepage through the dam was reduced as a result of this program; however, concrete deterioration has continued steadily since (MWH, 2007).

Since the dam cross section has been reduced by the ongoing concrete freeze-thaw deterioration, as-built construction drawings were not used for modeling the existing geometry of the dam. For reference, original drawings from 1913 and updates in 1967 are shown in **Appendix F**. Instead, sections of the dam's current geometry were developed from a point cloud created by a photogrammetry survey in April 2011, which recorded thousands of geometric points of the exposed dam faces in x, y, and z coordinates. The graphic viewer program, Quick Terrain Reader v7.1.4, plots these points in x, y, z coordinates, along with color data that was obtained at the time of the survey, in **Figure 11**. Data coordinates from the point cloud were imported into AutoCAD 2010, where contours of the dam's surface were developed at 10-foot intervals.

5.2 Reduced Section Geometry

Given that the outer layer of concrete of Salmon Creek Dam is so damaged by freeze-thaw deterioration, it cannot be considered to provide any strength in resisting applied loads. For example, the 1967 horizontal "H" cores indicate that a depth of at least 12-18 inches had deteriorated so much that recovery of the sample was limited and therefore no strength tests could be performed. Beyond about 18 inches for the next one to two feet, the concrete was deteriorated sufficiently to cause "fragmented" and "quite broken" core in many places. Discussion of the state of these cores may be found in **Appendix G**, in a series of letters from 1978.

Accordingly, the 1982 finite element analysis of the dam by IECO assumed a reduced section, where sound concrete was assumed at about a three foot depth for the upper 50 feet of the dam (both upstream and downstream faces) and about a two foot depth for the lower portion of the dam. IECO's reduced geometric section is shown in **Figure 12**, which is extracted from the original IECO report found in **Appendix E**.

Similarly, depth to solid concrete was estimated using the data from MWH's 2011 coring program, which is summarized in **Table 11**. Original detailed field logs from the 2011 coring program may be found in **Appendix H**. First, cross sections from the photogrammetry survey point cloud were taken at evenly spaced stations along the dam crest. The depth to solid concrete (2011 cores only) were superimposed on these cross sections, as shown in **Figures 13-16**. The depths shown accounted for the heavily deteriorated surface with voids and the layer of fractured concrete encountered during coring. The reduced section geometry (**Figure 12**) from 1982 was then compared to the 2011 corings at the crown cantilever (shown in **Figure 14**), and was further reduced in locations where heavier deterioration has occurred since 1982. This final reduced section used to create the FEM model is shown in **Figure 17**.

Thereafter, 10-foot contours that were initially developed in AutoCAD from the point cloud data were then offset a uniform distance based on the newly defined reduced section geometry. Two-dimensional cross sections of the crown cantilever and other stations from this reduction are shown in **Figure 18**, confirming consistency with the reduced section geometry.

Table 11. Depth to Solid Concrete, 2011 Coring Program

Core	Elevation (ft)	Total Core Length (in)	Depth to Solid Concrete (in)	**Notes on Core** *(#'s indicate sections from outside to inside of core)*
D252	1038	30	11	1) 6" (heavy fracturing); 2) 5" (light fracturing); 3) 19" (no visible fractures).
D451	1040	23	At surface	23" solid core, no fractures.
D251	1043	Unknown	Unknown	Numerous pieces, all crumbly and heavily fractured.
D312	1043	Unknown	Unknown	Largest portion of sample was 13" long. Heavy & hairline fractures.
D311	1046	24	*24***	1" extremely weathered, fractured all throughout length.
D241	1065	24	*14**	16" solid core, with light fracturing on outside end.
D441	1067	*25**	1	1) 1" fractured/broken; 2) 24" remaining good, no fractures.
D541	1077	37	*8**	1) 8" (contained 2 pieces, crumbly); 2) 20".
D231	1105	24	*15**	1) 3"; 2) 12" (light fracturing).
D531	1105	25	*5**	1) 5"; 2) 20". Pieces broke when removing.
D431	1111	36	12	1) 3" heavily fractured; 2) 8.5" light fracturing (broke when snapped); 3) 24" solid, no fracturing.
D121	1115	24	*24***	1) 7" (heavy fracturing); 2) Multiple pieces lightly fractured (4", 2", 3", 7").
D621	1115	*28**	12	1) 2" (heavy fracturing); 2) 10" (heavy fracturing); 3) 16" (no fracturing).
D221	1125	24	At surface	Removed as 21" long, no visible fracturing.
D421	1125	*24**	4	1) 4" rubble; 2) 20" good without fractures or defects.
D521	1125	24	*9**	1) 9"; 2) 15". Pieces broke when removing.
D112	1132	24	*24***	2nd attempt in vicinity. 1) Heavy fracturing (pieces 2", 3", 7"); 2) 9" (light fracturing).
D111	1135	29	*29***	Heavy fracturing (pieces 11", 2", 4", 7"). Inside of hole shows heavy fracturing.
D211	1135	36	18	1) 8" (light fracturing); 2) 10"; 3) 17" (no visible fracturing).
D511	1135	23	At surface	23" solid core, no fractures.
D612	1135	38	20	1) 4" Fractured; 2) 5" rubble; 3) 11" lightly fractured; 4) 17" no visible defects.
D411	1140	*32**	*32***	1) 4" weathered; 2) 6" heavy fracturing; 3) 6" rubble; 4) 16" microfractures & parts missing.
D611	1145	*41**	*41***	41" drilled into dam, with only rubble.
U441	1057	23	At surface	23" solid core, no fractures.

Core	Elevation (ft)	Total Core Length (in)	Depth to Solid Concrete (in)	**Notes on Core** *(#'s indicate sections from outside to inside of core)*
U541	1057	22	At surface	22" solid core, no fractures.
U241	1058	18	At surface	18" solid core, no fractures.
U231	1105	17	*17***	17" long, light fracturing in some locations.
U431	1105	*26**	*26***	1) 12" long (10" useable); 2) 8" piece; 3) 6" piece. All heavily fractured.
U531	1105	23	*2**	23" solid core. Void near outside end from embedded wood. Minor fractures near ends.
U121	1123	36	16	1) 10" (heavy fracturing); 2) 6"; 3) 17" (no visible fracturing).
U221	1125	30	*30***	1) 2"; 2) 6" (rubble); 3) 8" (heavy fracturing); 4) 14" (some fine fractures).
U521	1127	28	9	1) 9"; 2) 19" (no visible fractures).
U421	1128	40	20	1) 8" (air voids, wood pieces); 2) 10" with voids; 3) 2" with voids; 4) 20" (with 12" useable length).
U621	1129	28	7	1) 7" (light fracturing); 2) 20" (no visible fracturing).
U411	1141	*24**	*24***	1) 13" solid concrete; 2) continued 11" more: rubble. Concrete collapsing. Area too weak to drill other holes.
U111	1145	30	*30***	1) 9.5" (no visible fracturing); 2) 1.5"; 3) 10" (heavy fracturing).
U211	1145	26	6	1) 1"; 2) 3"; 3) 2"; 4) 18" (no visible fractures).
U511	1147	28	13	1) 13" (heavy fractures); 2) 15" (no visible fractures).
U611	1148	38	12	1) 2" (heavy fracturing); 2) 10" (light fracturing); 3) 25" (no visible fracturing).

Note: "D" = Downstream cores, "U" = Upstream cores.

** Estimated dimension from notes.* *** Entire depth of core shows fracturing.*

5.3 Finite Element Model

The three-dimensional static, linear, and non-linear dynamic finite element analyses of Salmon Creek Dam were performed using the computer program ANSYS Version 14.0. ANSYS is a state-of-the-art commercially available general finite element method (FEM) program, which is widely used as a research and development tool in a number of industries, including a variety of civil/structural engineering applications, including static and dynamic stability evaluations of dams.

The reduced section geometry of the dam was imported from AutoCAD into ANSYS, and subsequently used as the basis for creating the FEM mesh. A combination of the automated meshing capabilities of ANSYS and specified mesh densities were utilized to model the site geometry and the dam structure in the finite element model. The nonlinear finite element model consisted of 30,160 elements and 33,153 nodes. Mostly hexagonal (“brick”) elements were used, while prism (“wedge”) elements were utilized in portions of the model where the geometry was not regular. The dam and rock foundation elements used in the model consisted of 8-node elements, with one node at each corner. Three-dimensional mass elements (added mass) attached to the nodes of the elements on the upstream face of the dam were used to simulate hydrodynamic effects of the reservoir. The weights of the added masses on the dam face were computed based on Westergaard’s added mass approach (Zangar, 1952).

The FEM model of the dam has between two to five elements in thickness and 17 vertical rows of elements at the crown cantilever. The rock foundation block in the model extends three times the height of the dam in all directions. The elements of the dam-foundation contact are connected at the surface of the foundation elements (i.e., no embedment). The model geometry looking downstream is shown in **Figure 19** and looking upstream, including contact surfaces, in **Figure 20**.

To model nonlinearity of the dam, contact surfaces were created at each contraction joint, between the foundation and the bottom of the dam, and at the spillway. The ANSYS contact element is used to represent contact and sliding between 3-D "target" surfaces and a deformable surface, defined by this element. The element is applicable to 3-D structural and coupled field contact analyses. The element has the same geometric characteristics as the solid or shell element face with which it is connected. Contact occurs when the element surface penetrates one of the target segment elements on a specified target surface. Coulomb friction, shear stress friction, and user-defined friction can be used (coulomb friction is used in the current analysis). The element also allows separation of bonded contact to simulate interface delamination (i.e., joint opening) (ANSYS, 2011).

A nonlinear model of the dam allows redistribution of stresses throughout the dam and foundation, due to the ability of the contraction joints to open and close during dynamic loading, and transfer of stress from the dam to the foundation. These contact surfaces may be seen at the bottom of **Figure 20,** which are at the boundary of the transition from light to dark gray color shown in the mesh of the dam (**Figures 19** and **20**). Contact surfaces are created by having coincident, paired nodes and elements at the surface interface. With this nodal separation at each contact surface, each joint is allowed to move freely during dynamic loading, and allow for the relief of stress concentrations at the dam and the foundation contact. A cohesion of zero was specified at the interface of all contacts. Likewise, the model assumed a friction angle of 45°, and a friction coefficient of 1 at the contacts. It should be noted that stress relief due to nonlinear *material* properties (e.g., concrete yield and cracking models) was <u>not</u> included in this analysis.

The rock foundation of the FEM model was assigned stiffness only with no mass, consistent with the selected elastic (deformation) modulus zones identified from the previous evaluation (Section 4.8). The massless foundation allows for transmission of the seismic ground motion time history from the boundary of the model to the dam foundation, avoiding the inertial effects of the foundation mass that conservatively transmit additional energy and overestimate the force applied to the dam. Although the use of a massless foundation is a proven method to apply seismic energy to the dam model, reflection of the seismic waves at the boundaries of the foundation model tend to "trap" some of the seismic energy, which in turn is re-transmitted into the dam model. This reflection effect has been found to slightly overestimate stresses in dam models (~5% to 10%) when compared to infinite mass models that account for radiation damping and no reflection at the foundation boundaries (Zhang, 1998).

In order to reduce the overestimation of stress from wave reflection at the FEM foundation model boundary, modeling of the dam in computer program LS-Dyna was investigated. LS-Dyna is finite element software program that solves the finite element matrix equations explicitly for force equal to mass times acceleration (as opposed to ANSYS that provides an *implicit* stiffness matrix solution) and includes non-reflecting boundary elements that reduce wave reflection. However, the additional effort in developing a new model in a separate FEM program was weighed against the possibility of a nominal reduction in overall stress in the dam, where ultimately it was determined that the significant effort would have provided a nominal benefit when compared against the results of the non-linear model analyzed in ANSYS. This consideration was further reinforced due to the relatively small area of contact of the arch dam to the foundation, which meant that a substantial portion of the additional energy from reflected seismic waves would not be transmitted into the model. As such, the non-linear ANSYS FEM model was selected as the primary model to use in the evaluation of Salmon Creek Dam, since it was considered to provide an acceptable level of conservatism, while providing a relatively accurate representation of the dam's response to earthquake ground motion input.

5.4 Ground Motion Input

Three ground motions were used in this finite element analysis, and were developed as part of the seismic hazard analysis performed by MWH as part of this report, which is attached in **Appendix A**. The three selected ground motions are referenced throughout this report as follows:

- *Hector Mine*, a scaled ground motion – labeled "Earthquake 1."

- *Sitka Scaled*, a scaled ground motion – labeled "Earthquake 2."
- *Sitka Spectrally Matched*, a spectrally matched ground motion with similar accelerations to the earthquake, "Sitka Scaled" – labeled "Earthquake 3."

The acceleration time histories used in the analysis may be found in **Figures 30-34** of **Appendix A**.

5.5 Model Boundary Conditions

The static analysis model (i.e., reservoir pressure, uplift pressure, gravity, and temperature) boundary conditions included fixed nodes at the outer boundary of the foundation block. The boundary conditions at those nodes were fixed such that translation in the x, y and z coordinates was zero. The dynamic analysis model included static conditions at the initial step, and then the selected earthquake time-histories were applied at each boundary foundation node as velocities.

5.6 Static Analysis

The loads for the static loading are discussed below.

5.6.1 Gravity Loading

The gravity load was applied as a gravitational acceleration of 32.2 ft/sec^2. The weight of the dam is based on the average density of the concrete (155.7 lbs/ft^3). No gravity loads from the foundation were included, as the foundation elements were assumed to be massless, and provided only stiffness in the model.

5.6.2 Reservoir Hydrostatic Pressure Loading

The hydrostatic reservoir load was applied in the model as a distributed force load on the dam face based on the maximum normal operating pool reservoir condition at the FERC restricted level of El. 1140 feet. No flood, overtopping, or any other reservoir level fluctuation and resulting load combination was considered in the dynamic analysis. A separate probable maximum flood (PMF) loading condition was evaluated with hydrostatic load applied to El. 1170 and is discussed in section 6.3.

5.6.3 Uplift Pressure Loading

Uplift pressures were applied at the dam-foundation interface as a distributed force load, based on depth and width of the dam's cross section at each location. Uplift pressures were applied as surface loads on areas at the interface. A maximum pressure was applied on each interface area's upstream edge, and varied linearly from upstream (maximum) to downstream (zero) for each cross section under consideration.

5.6.4 Temperature Loading

5.6.4.1 Air Temperature and Wind Speed

Using an estimated annual temperature cycle, a cyclic ambient temperature load was applied on the dam to create a typical temperature distribution through the dam cross section. The historical temperatures used to create the temperature loading were based on the nearest weather station to Salmon Creek Dam, which is located downstream of the dam in Juneau (**Figure 21**). Temperature and wind speed data collected from the weather station is shown below in **Table 12**.

Table 12. Average Monthly Temperature & Wind Speed at AKDOT Weather Station – Juneau, AK

Month	2008		2009		2010		2011	
	Average Temp (°F)	Average Wind Speed (mph)	Average Temp (°F)	Average Wind Speed (mph)	Average Temp (°F)	Average Wind Speed (mph)	Average Temp (°F)	Average Wind Speed (mph)
January	27.6	1.1	27.0	2.4	31.8		33.3	
February	28.4	0.5	30.5	2.2	37.8		27.2	1.8
March	35.1	2.8	30.8	0.8	37.1		30.6	
April	38.5	0.9	39.0		42.1	2.1	39.9	1.9
May	48.2	4.3	48.6	1.8	51.1	3.5	51.3	
June	51.0	4.2	55.3	1.2	53.8	3.7	54.4	
July	52.1	2.6	60.9		54.6	3.8	56.2	2.1
August	53.6		56.0		57.5	2.2	53.4	3.5
September	49.6	3.2	51.4		52.3	1.6	49.9	2.8
October	41.6	3.0	43.2	1.8			43.0	2.7
November	36.7	2.0	34.1				30.2	
December	25.5	1.7	29.5				34.7	

This weather station is located approximately 2.5 miles from the project site at El. 16 feet, however, the dam is located at a higher elevation (average El. 1090 ft). Therefore, the average monthly temperatures were corrected for the elevation difference. The correction was made by reducing the average monthly temperatures by 1°F for each 250 feet gained in elevation based on the guidance in USBR Monograph No. 34 (USBR, 1981). These calculations are shown below, and the adjusted temperatures are shown in the following table, **Table 13**.

$$\textit{Difference in Elevation} = 1090\,ft - 16\,ft = 1074\,ft$$

$$1074\,ft / 250\,ft = 4.3°F$$

Table 13. Adjusted Average Monthly Temperatures for Salmon Creek Dam

Month	Recorded Average Monthly Temp (°F)	Adjusted Average Monthly Temp (°F)
January	29.9	25.6
February	31.0	26.7
March	33.4	29.1
April	39.9	35.6
May	49.8	45.5
June	53.6	49.3
July	56.0	51.7
August	55.1	50.8
September	50.8	46.5
October	42.6	38.3
November	33.7	29.4
December	29.9	25.6

The average annual adjusted temperature for the dam site is 37.8°F, and the average annual wind speed is 2.3 mph.

5.6.4.2 Convection (Film) Coefficient

The convection (film) coefficient for concrete and rock surfaces exposed to air was calculated for the average annual wind speed of 2.3 mph. Computation of the film coefficient is based on the U.S. Army Corps of Engineers ETL-1110-2-365 methodology, which is summarized below (USACE, 1994).

$$h = 0.1132V^{0.8} \quad \text{for } V > 10.9 \text{ mph} \tag{A-2}$$

and

$$h = 0.165 + 0.0513(V) \quad \text{for } V < 10.9 \text{ mph} \tag{A-3}$$

where,

$$h = \text{film coefficient}\left(\frac{Btu}{day - in.^2 - {}^\circ F}\right)$$

$$V = \text{wind velocity}(mph)$$

The film coefficient calculated for surfaces exposed to air is 1.7 BTU/hr-ft^2-°F. The convection coefficient for concrete and rock surfaces exposed to reservoir water was 61.4 BTU/hr-ft^2-°F (Berga et. al, 2003).

5.6.4.3 Reservoir Temperatures

The temperatures from the surface to the bottom of the reservoir were estimated and included in the thermal analysis. Since no temperature data is available for Salmon Creek Reservoir, temperature distributions in reservoirs from other dams were applied. The reservoir temperature distribution from a recent project, the San Vicente Dam Raise project, is shown for reference in **Figure 22** along with the temperature profile developed for Salmon Creek Reservoir. It should be noted that, although the near surface reservoir temperatures at San Vicente fall within a warmer temperature range, the fluctuation of reservoir temperature in the upper 40 to 60 feet is typical at most reservoirs. The temperatures in the reservoir at Salmon Creek Dam were adjusted accordingly to match the annual ambient air temperature ranges at the surface.

5.6.4.4 Material Thermal Properties

The concrete and rock thermal properties were estimated using typical values reported by USBR, shown in **Table 14** (USBR, 2006).

Table 14. Material Thermal Conductivity Properties

Material	*Thermal Conductivity (BTU/ft-hr-°F)*	*Specific Heat (BTU/lb-°F)*
Foundation Rock	1.63	0.232
Concrete	1.52	0.23

5.6.4.5 Thermal Analysis Conditions

The temperatures listed above in **Table 13** were used as the basis for performing a cyclic thermal analysis to establish a typical temperature distribution through the dam cross-section, where the typical "winter" and "summer" thermal states of the dam were selected and used in the structural analyses. In order to achieve a steady state cyclic temperature distribution, the thermal analysis was run over a period of four years. The coldest winter temperature (found to be in December and January) was then applied in the static analysis, before the dynamic loads were applied.

5.7 Dynamic Analysis

The loads in the dynamic analysis consisted of the ground motion velocity time histories and hydrodynamic reservoir loading on the upstream face of the dam.

5.7.1 Ground Motion Input

The ground motion velocity time histories were applied to all of the boundary nodes of the foundation block. Each time history was 29.99 seconds in length, which includes the most intense time of each earthquake. Two horizontal velocity time histories were applied in the upstream-downstream, and the cross-canyon directions. The third acceleration time history was applied in the vertical direction.

5.7.2 Hydrodynamic Reservoir Loading

Hydrodynamic reservoir loading from the reservoir on the upstream face of the dam was estimated based on the surface area below El. 1140 and orientation of each element using the Westergaard method (Zangar, 1952) and applied to the model as added masses attached to the upstream nodes for the full reservoir condition (El. 1140).

5.7.3 Dynamic Analysis Cases

Three earthquake ground motions were selected to evaluate the range of dynamic response of the dam and are documented in independent load cases or scenarios. Further, in order to evaluate the response of the dam through changes to analysis method (linear vs. non-linear), material properties, and initial condition static loading, several scenarios were run for comparison while fixing the earthquake loading condition (Sitka Spectrally Matched earthquake). A damping ratio of 5% was applied to all analyses. The six scenarios are described in the following table, **Table 15**.

Table 15. Finite Element Analysis Load Case Scenarios

Scenario Number	*Earthquake*	*Description of Analysis*
1	Hector Mine Scaled	Nonlinear
2	Sitka Scaled	Nonlinear
3a	Sitka Spectrally Matched	Linear
3b	Sitka Spectrally Matched	Nonlinear with Zoned Material Properties
3c	Sitka Spectrally Matched	Nonlinear
3d	Sitka Spectrally Matched	Nonlinear with No Temperature Included

5.8 Analysis Procedure

A modal analysis was performed using the selected material properties (uniform for the entire dam) to calculate the fundamental periods of vibration and mode shapes of the linear model of the dam, which were compared to the measured ambient vibration modal frequencies developed in 1982. The fundamental periods of vibration are compared in **Table 16** below and are plotted in **Figure 23**.

Table 16. Fundamental Modal Frequencies and Periods of Vibration

	2012 Modal Analysis Reservoir El. 1140		1982 Modal Analysis Reservoir El. 1137.2		1982 Ambient Vibration Survey Reservoir El. 1137.2	
Mode #	*Frequency (Hz)*	*Modal Period (sec)*	*Frequency (Hz)*	*Modal Period (sec)*	*Frequency (Hz)*	*Modal Period (sec)*
1	4.94	0.203	5.10	0.196	5.30	0.189
2	5.75	0.174	5.35	0.187	6.50	0.154
3	7.42	0.135	7.04	0.142		
4	8.82	0.113	8.47	0.118		
5	10.09	0.099	9.60	0.104		
6	10.14	0.099	10.35	0.097		
7	11.32	0.088	10.61	0.094		
8	11.62	0.086	11.05	0.090		
9	12.49	0.080	11.23	0.089		
10	13.08	0.076	11.70	0.085		

As shown in **Table 16** and **Figure 23**, the fundamental periods of vibration and mode shapes produced in the current FEM model provide a reasonable match to the measured frequencies from 1982, providing confirmation that selected material properties are appropriate for modeling linear dynamic response of the dam. It should be noted that non-linear dynamic analysis does not rely on frequency response computed in a modal analysis. Nevertheless, this comparison provides a check on whether the selected material properties are appropriate for the analyses.

Upon selection and confirmation of material properties, the suite of dynamic analyses from **Table 15** was initiated. The first step in each dynamic analysis develops the static loading conditions in the dam before the earthquake time history loading is applied. The static analysis is performed during the first few time steps of each earthquake run (at time less than 0.005 seconds), and then the dynamic analysis is started at time 0.01 seconds. For the non-linear models, time-steps were allowed to vary between a minimum of 0.0005 seconds and a maximum of 0.01 seconds, depending upon solution convergence at each time step, throughout each earthquake time history from 0.01 to 29.99 seconds.

The solution output was then investigated to find the maximum stresses in the dam. Stress time histories were plotted for over 100 nodes on the upstream and downstream faces of the dam. Using stress peaks indicated in the time histories, nodal stress contour plots were plotted in order to further investigate locations of higher stress in the dam. Additional results were also considered in the evaluation of the response of the dam, including nodal displacement and contact status of coincident nodes at the vertical and horizontal joints of the non-linear analyses. Results are presented and discussed in Section 6.0.

6.0 STRUCTURAL STABILITY ANALYSIS RESULTS

The results from 3D FEM stability analyses of Salmon Creek Dam are presented in the following sections.

6.1 Dynamic Analysis

The following time history results were extracted from each dynamic analysis load case scenario:

- principal tensile stress
- principal compressive stress
- relative displacement in the y-direction (upstream-downstream)
- comparison of applied accelerations to resultant boundary nodal accelerations
- relative displacement between coincident contraction joint nodes
- contraction joint contact status
- contraction joint gap distance

These results were extracted from a series of nodes selected along regularly spaced elevation intervals on each face of the dam (**Figures 19 & 20**). The results are reported as follows:

- **Figures 24-52** for Earthquake 1: Hector Mine Scaled, Standard Nonlinear Analysis
- **Figures 53-81** for Earthquake 2: Sitka Scaled, Standard Nonlinear Analysis
- **Figures 82-104** for Earthquake 3: Sitka Spectrally Matched (SM), Linear Analysis
- **Figures 105-133** for Earthquake 3: Sitka Spectrally Matched, Nonlinear Analysis with Zoned Material Properties
- **Figures 134-162** for Earthquake 3: Sitka Spectrally Matched, Standard Nonlinear Analysis
- **Figures 163-191** for Earthquake 3: Sitka Spectrally Matched, Nonlinear Analysis with No Temperature Included in Analysis

Snapshots of the principal tensile stresses at the times of maximum stress excursions identified from the time histories are included in **Figures 192-195**.

6.1.1 Maximum Stresses

Table 17 provides a summary of the maximum principal tensile and compressive stresses in the dam for each load case scenario. **Figure 196** depicts the nodes that correspond to the listed stress excursions.

Table 17. Maximum Dynamic Stresses

Dynamic Tensile Strength = 346 psi *Dynamic Compr. Strength = 4334 psi*		Max. Principal Tensile Stress (psi)			Max. Principal Compressive Stress (psi)
Load Case	Analysis Type	Crest(1)	Above HWL*(2)	Below HWL*(3)	Overall Maximum(6)
(1) Hector Mine	Nonlinear	544	443	390(4)	876
(2) Sitka Scaled	Nonlinear	643	509	499	1183
(3a) Sitka SM	Linear	641	533	684(5)	683(7)
(3b) Sitka SM	Nonlinear, Zoned Matl. Props.	595	496	460	1217
(3c) Sitka SM	Nonlinear	611	499	454	1189
(3d) Sitka SM	Nonlinear, No Temperature	411	338	273	1013

* HWL is high water level, El. 1140.

(1) Greater than El. 1170. Maximum occurs at **Node 2045** (upstream face, El. 1175).

(2) Greater than or Equal to El. 1140 and Less than or Equal to El. 1170. Maximum occurs at **Node 2018** (upstream face, El. 1170).

(3) Less than El. 1140. Maximum occurs at **Node 1004** (downstream face, El. 1080).

(4) Maximum occurs at **Node 1346** (downstream face, El. 1100).

(5) Maximum occurs at **Node 140** (upstream face, El. 1030).

(6) Overall maximum occurs at **Node 109** (downstream face, El. 1020).

(7) Maximum occurs at **Node 362** (downstream face, El. 1040).

As seen in **Table 17**, the maximum principal compressive stress in the dam during all runs is well below the estimated compressive capacity range for the concrete. The maximum principal compressive stress of 1217 psi occurs at Node 109 at El. 1030; the earthquake compressive stress time history for this node is shown in **Figure 121**.

The linear run, using the Sitka SM earthquake time histories, shows the highest overall tensile stresses, particularly below the reservoir level. This linear run is more conservative than non-linear analyses, which redistribute stresses through incorporation of joints. It is more useful to consider the non-linear analyses, as they are more representative of the dam's behavior during a seismic event.

Of the three non-linear earthquake runs (Hector Mine, Sitka Scaled, and Sitka SM), the Sitka Scaled earthquake exhibited the highest maximum principal tensile stress, while the Sitka spectrally matched (SM) earthquake showed the highest maximum principal compressive stress. Stresses for load case 3b (zoned model) were similar to those exhibited in the standard non-linear Sitka SM run. The highest principal tensile stress (499 psi) at or below reservoir normal pool elevation is found in case 2 (Sitka Scaled) at node 1004 at El. 1080.

6.1.2 Tensile Stress Excursions

Excluding the linear model load case 3a, the high tensile stress excursions found at node 1004 at El. 1080 near the vertical contraction joint on the left side of the dam (looking upstream) are plotted in **Figures 197-201,** showing stress time-histories, and principal stress contour and vector plots at peak excursions. These plots indicate that the tensile stresses in this area are vertical "cantilever" stresses that could potentially cause a horizontal crack to initiate at the concrete surface, depending on the assumed dynamic tensile capacity of the concrete at this location, which is assumed to range between 350 to 450 psi. The maximum number of tensile stress excursions occurring in each load case scenario is summarized in **Table 18** below. It should be noted that in **Figure 200**, no stress excursions occur for load case 3d (no temperature load). Additional discussion regarding temperature load is discussed at the end of this section

Table 18. Number of Tensile Stress Excursions*

	Crest	Near CJ[1]	Upstream Nodes			Downstream Nodes		
Node Number	2045	1004	2018	1838	140	2028	1848	1597
Elevation	*1175*	*1080*	*1170*	*1140*	*1030*	*1170*	*1140*	*1120*
Load Case	Number of Tensile Stress Excursions							
(1) Hector Mine, Nonlinear	6	2[2]	3	0	0	2	0	0
(2) Sitka Scaled, Nonlinear	18	3	9	0	0	8	0	2
(3a) Sitka SM, Linear	23	N/A	10	8	38	7	0	0
(3b) Sitka SM, Nonlinear, Zoned Matl. Props.	16	5	4	1	0	5	0	1
(3c) Sitka SM, Nonlinear	16	5	6	1	0	5	0	1
(3d) Sitka SM, Nonlinear, No Temperature	3	0	0	0	0	0	0	0

* Reports number of principal stress excursions above the lower bound of the estimated dynamic tensile strength capacity of the concrete, 346 psi.

(1) CJ = contraction joint.
(2) Node under consideration is **Node 1346** (downstream face, El. 1100).

As can be seen in **Table 18** and the stress time histories, there are multiple instances where stress excursions occur above the lower bound of the estimated tensile capacity range. Overall, the Hector Mine earthquake showed the fewest excursions, when compared to the other nonlinear models, Sitka Scaled and Sitka SM. Likewise, no excursions were seen at the nodes under consideration for the Sitka SM run without temperature included in the analysis.

Tensile stress excursions above the lower bound tensile capacity primarily occur on nodes above the reservoir normal pool El. 1140, although several excursions are also seen at reservoir level (El. 1140) or below on the upstream face of the dam. In the linear Sitka SM run (load case scenario 3a), a high number of excursions, 38, were seen below reservoir level at Node 140, which is at the contact with the foundation at El. 1030. High stresses at or near the dam-foundation contact are expected due to the singularity caused by the sharp transition in geometry from the dam to a horizontal foundation surface. This singularity is relieved by opening and closing of this interface (or within the fractured foundation rock mass) during earthquake loading. Joints are modeled at the dam-foundation interface in the non-linear analyses and thus allow for this stress to be relaxed through joint opening and closing.

6.1.3 Contact Element Status

Contact status reported in the Figures is generated based on the default ANSYS settings, where the following 3 statuses are defined:

1. Closed and Sticking – The contact pairs (joint) are in contact and no movement occurs along the joint.

2. Closed and Sliding – The contact pairs (joint) are in contact and but are moving along the joint.

3. Open but Near Contact – The contact pairs (joint) have separated by greater than -0.02 inches, but are near contact within the default 3-D “pinball” region of contact around each node or element. The default pinball region in the current analysis is defined as the 2 times adjacent element size, or generally around 20 feet.

Based on the criteria defined above, the “open, near contact” region is reached at many timesteps during the earthquake simulation, as shown for the contact status in the Figures (**Figures 49, 50, 78, 79, 130, 131, 159, 160, 188, and 189**). Evaluation of the coincident nodes at these contacts shows that the gap distance is always less than 0.4 inches (**Figures 51, 52, 80, 81, 132, 133, 161, 162, 190, 191**).

It should be noted that the initial condition of coincident nodes at the joint-foundation interface are “closed and sticking,” as would be expected. This initial condition occurs when only gravity is applied as a static load. Subsequently, when the remaining static loads (hydrostatic, winter temperature, and uplift) are applied, a minor increase in gap distance is seen. In this case, the contact status is shown to be "open, near contact" during this initial static loading condition, implying that joints are open prior to earthquake loading. Rather, when looking closer at the gap distances (in the Figures mentioned above), it is clear that the joints are effectively closed, but are shown to be open due to the small tolerance of 0.02" opening and high level of accuracy (i.e., significant digits) computed in the model.

6.1.4 Discussion of Impact of Temperature Load on Non-linear Dynamic Results

Of particular note is the Sitka SM load case scenario 3d (no temperature loads applied), where the earthquake analysis results show only two minor excursions above tensile capacity at the crest, node 2045 at El. 1175, the larger of which is 412 psi (**Figure 163**). Overall, load case scenario 3d displays much lower stresses as compared to the other non-linear load case scenarios. A direct comparison between load case scenario 3c and 3d in **Figure 202** (which only differs by whether temperature load was applied) shows the magnitude of the increase in tensile stress at node 2018 (El. 1170).

Due to the significant change in stress noted between these two load cases, stresses imposed by temperature loads were further analyzed. Stresses from the static load cases with and without temperature loads are plotted in **Figures 203 & 204**. These figures plot the tensile stress contours and compare stresses from selected nodes to stresses computed from a balance temperature computation performed in accordance with USACE ETL-1110-2-542 (USACE, 1997).

The balance temperature computation, which estimates stresses based on internal restraint imposed by the temperature differential through the dam cross-section, more accurately estimates thermal stresses in upper portions of the arch dam; detailed balance temperature calculations are included in **Appendix I**. The impacts of external restraint (i.e., the foundation) are considered nominal once the length to height ratio of the base restraint to height in dam is less than 1.0, except points at 10% of the total height and below. In contrast, the standard method of computing thermal stress in concrete dams is achieved by computing strains using a differential of temperature (ΔT) from the "stress free," or average annual, temperature times the coefficient of thermal expansion (CTE).

$$Strain, \varepsilon = (\Delta T)(CTE)$$

As shown in **Figure 204,** the comparison of the balance temperature against stresses computed within ANSYS using the above formula shows that the use of the single "stress free" temperature overestimates the expected thermal stresses in the dam when compared to balance temperature calculations. This overestimation of thermal stress at higher elevations in the dam is due to the current limitations of the computational methodologies within the FEM model; a more accurate representation of the thermal stress state is not possible. By comparison, the balance temperature calculations do not incorporate stresses imposed by external foundation restraint, which are considered negligible at heights of 50% of the dam or greater above the foundation. Given the difference between the more accurate balance temperature calculations and the simplified temperature stress computation methodology in the FEM model, the results of the non-linear FEM analyses with and without temperature load are therefore used to surmise an overall judgment on the predicted response of the dam under earthquake loading in the following section.

6.2 Seismic Structural Analysis Findings

The seismic stability evaluation of Salmon Creek Dam utilized linear elastic and non-linear 3D FEM analyses under design earthquake loading, utilizing several load case scenarios to evaluate sensitivity of the dam response. The results of the analyses (Tables 17 and 18) show that the estimated tensile capacity of the dam concrete may be exceeded up to sixteen times during the Sitka Spectrally Matched design earthquake at the dam crest (El. 1175) for the non-linear model (case 3c) and up to twenty-three times for the linear model (case 3a). The linear model also showed the most stress excursions at or below the reservoir pool level at a total of eight excursions. The extent and number of stress excursions in the linear model exceed those of the non-linear model cases due to the fact that the linear model does not model vertical contraction joints or joints at the dam-foundation contact, which relieve and redistribute tensile stresses. Thus, the linear model results are considered for comparative purposes only; in particular, the linear model is useful for confirming whether the selected material properties for the model match the measured field vibration surveys (Section 5.8).

The non-linear model load case scenario (load case scenarios 1, 2, 3b, 3c and 3d) results showed fewer excursions at lower stress, and included about five excursions at or below the reservoir level (El. 1140) in cases 2 and 3b. The excursions below the crest level were found to be surficial, not extending through the dam thickness, and well within 5% of the dam surface area and thus were found to be acceptable per Chapter 11 of FERC's Engineering Guidelines for Evaluation of Hydropower Projects (FERC, 1999), which state that five excursions or less within 5% of the dam surface area are acceptable. Also, when considering the lowest range of possible response of the dam in load case scenario 3d (no temperature load applied), the dam shows no tensile stress excursions below normal pool elevation El. 1140. Given the evaluation of the temperature load described in Section 6.1.4, it is anticipated that the actual dam response under the maximum earthquake load will be somewhere between load case scenario 3d and the remaining load cases. Moreover, when considering that the ANSYS non-linear model results are somewhat conservative (Section 5.3), the anticipated level of tensile stress in the dam is expected to be roughly 5% to 10% lower. As a result, the number of possible stress excursions at the crest in case 2 is expected to fall from a maximum of 18 to roughly one half, or about nine, and would fall within an acceptable range that is generally in conformance with FERC Guidelines (FERC, 1999). Similarly, the magnitude of the single 369 psi excursion at reservoir level in load case scenario 3c is expected to be below 346 psi.

6.3 Probable Maximum Flood Static Analysis

In order to evaluate stresses in the reduced-section dam under extreme static load, an additional analysis was performed for the probable maximum flood (PMF) loading condition in the non-linear FEM model of the dam. The PMF used in the structural stability analysis is based on the latest PMF routing, which utilized the 1987 HEC-1 hydrograph developed from the Hydrometeorological Report No. 54 (HMR 54) by the National Weather Service and the current operating level of the reservoir, El. 1140. The PMF routing resulted in a maximum reservoir level of El. 1166.9 (MWH, 2007) in a late summer/early fall storm.

Since the dam is modeled at 10-ft contours in ANSYS, the resulting element divisions are at even 10-foot increments and therefore the hydrostatic loading for the PMF was applied starting at El. 1170. Thermal loading during the PMF is based on late-summer conditions, where temperatures on September 1st from the thermal model were applied to the structural model. Also included were uplift, gravity, and hydrostatic pressures to complete static PMF loading case. In order to evaluate the impacts of the simplified temperature loading on the model, the static loading described above was combined to create two PMF loading cases, one model with all static loads and a second without late summer temperature.

As seen in **Figure 205**, the principal tensile stresses on the upstream and downstream faces of the dam are all within the tensile capacity of the concrete for both the no temperature and late summer temperature PMF load cases. On the downstream face of the dam, the tensile stresses are below 80 psi, and on the upstream face of the dam, the tensile stresses are below100 psi.

Figure 206 compares the upstream-downstream displacement of the dam under the PMF load case to the normal pool level load case, both with and without temperature included in the model. The normal pool reservoir condition was modeled with winter temperatures, thus displacements and coutours slightly vary from the PMF results. However, displacement results for the load cases shown are typical and show an expected increase in displacement near the crest for reservoir El. 1170.

7.0 SUMMARY, CONCLUSIONS AND RECOMMENDATIONS

This section provides a summary, conclusions, and recommendations which are made based on the findings of the data review, seismic hazard assessment, and the 3D FEM structural evaluation of Salmon Creek Dam.

7.1 Summary

7.1.1 Existing Dam Concrete Condition and Material Properties

Current surveys and investigations were reviewed in conjunction with historic data and correspondence in order to assess and determine the current condition of the dam. Review of the historic information provided the general location of the vertical joints in the dam, construction methods for assessing variability of the concrete strength throughout the dam, extent and location of upstream face rehabilitation in 1967, and data from previous concrete coring and testing programs.

Survey data from the 2011 survey using photogrammetric techniques was used to generate cross sections of the dam and compared against the as-built conditions and previously assumed deterioration. Based on the comparison, it was found that the overall loss in cross section through 2011 was similar to the assumption made in 1982 that assumed lost concrete and a layer of low strength concrete. Similarly, the cross section of concrete that was assumed of sufficient strength for the current analyses incorporated the physical loss of concrete determined by the photogrammetry survey and an additional depth of deteriorated, low strength concrete. The depth was estimated using the recent 2011 core log data, resulting in a two- to three-foot additional loss in cross section, compared to the 1982 analysis, over a 30-foot height on the upstream face between El. 1090 to El. 1120, or about 65 feet from the dam crest.

Detailed comparison of 1967, 1982 and 2011 concrete testing results revealed differences in average values and testing methods between programs, which ultimately required judgment in establishing material properties and threshold strength values for the FEM analyses. A range of material properties was selected for use in sensitivity analyses. Similarly, a range of threshold values was selected for use in determining potentially overstressed areas in the dam.

7.1.2 Seismic Hazard Assessment

An updated seismic hazard assessment (SHA) performed for the project site evaluated regional geologic setting, characterized seismic sources, provided recommendations for the maximum credible earthquake and included recommended earthquake time histories for the FEM analyses of the dam. Three earthquake time histories were selected based on their source characteristics and scaled or modified to match the selected site response spectrum. The results from the SHA reduced the anticipated peak ground acceleration from 0.35g in the previous analysis (JMM, 1983) to 0.18g, and from a magnitude 8.0 earthquake at 34 km to a magnitude 7.3 at 53 km.

7.1.3 Structural Stability Analyses

Using the selected range of material properties and earthquakes, six seismic load case scenarios were developed to evaluate the sensitivity of response of the dam under dynamic earthquake loading. As shown in the stress contour snapshots (Figures 197-201), the brief stress excursions above the estimated tensile capacity of the concrete were encountered in multiple load case scenarios, occurring in localized areas of the dam and generally above the reservoir level. Evaluation of the stress excursions show that they are limited in extent, occur mostly within the estimated dynamic tensile stress capacity range of the dam (346 psi to 505 psi), and are very brief and surficial. Most excursions meet criteria defined by FERC (FERC, 1999), where excursions occur over less than 5% of the dam area and generally occur five times or less at a given node. Moreover, upon further comparison of the load case scenarios with or without temperature load, it was determined that the level of stress and number of stress excursions at or below reservoir level will be limited or below the lowest estimated concrete tensile capacity.

The PMF load case evaluation that utilized the latest PMF maximum pool level at El. 1167 demonstrated that peak tensile stresses generated within the dam do not exceed 100 psi and thus are well within the tensile capacity of the concrete by a factor greater than 2.

7.2 Conclusions

The evaluation of the concrete testing results indicated a possible declining trend in the strength of the concrete. The deterioration of the outer layer of concrete in the dam has been attributed to freeze-thaw weathering. History shows that the weathering has continued over time with an associated loss of cross section of the dam. These conditions will likely continue without mitigation. Therefore, given these observations and that the 2011 cores were tested in full accordance with current ASTM standards, it was determined to use the current coring and testing data as the basis for the material properties used in this study.

A re-evaluation of the site seismicity was performed and results indicated that a decrease in the peak ground acceleration at the site from previous studies. This reduction in the anticipated site response is based on updated ground motion attenuation relationships and the overall advancements in seismological practice that incorporate both probabilistic and deterministic methods to determine site response from an aggregated source of known seismicity.

Dynamic stress analyses of the dam demonstrated a potential for cracks to form in the higher elevations of the dam near the crest under the MCE loading. Conservatively, these cracks could extend a few feet down from the dam crest. The assumption of cracking is based on the conservative evaluation built into the ANSYS FEM model that applies an overestimated temperature load and massless foundation that reflects seismic energy and increases seismic load on the dam. However, given the current condition of the dam, it is possible that spalls and/or chucks of concrete could detach from the dam, causing damage to the outlet works and possibly rupture the outlet pipe leading to an uncontrolled release of the reservoir.

Under PMF loading, the crest of the dam is expected to deflect downstream approximately an additional 0.4” and a maximum tensile stress up to 100 psi. Considering the most recent testing and evaluation of concrete strengths, it is expected that the dam will withstand the additional hyrdrostatic load from the PMF reservoir pool at El. 1167.

Given the current reservoir level restriction, a sudden, uncontrolled release of the reservoir from overtopping is considered unlikely due to a partial failure of the dam in the upper elevations. A total failure of the dam under the maximum credible earthquake loading is considered unlikely during or post-earthquake. Repairs of the dam may be required following a major earthquake event affecting the dam.

7.3 Recommendations

Based on the evaluation results, the following recommendations are provided:

1. A new Potential Failure Mode (PFM) should be included in the next FERC Part 12D five year inspection report for the case of the outlet pipe being damaged by falling debris from the dam during a large earthquake leading to a partial or sudden and uncontrolled release of the reservoir. It is also recommended that remediation of localized concrete failures should be studied to prevent possible damage to or rupture of the outlet works.

2. A regular program of sampling cores from the dam, laboratory testing the concrete and surveys of the dam surfaces should be considered for comparison with the findings of this study on a ten year schedule. The need for updated seismic hazard assessments and stress analyses should also be examined as part of the ten year review.

8.0 REFERENCES

American Concrete Institute (ACI), 2005, *Building Code Requirements for Structural Concrete (ACI 318)*, ACI Committee 318.

ANSYS Mechanical, A General Purpose Finite Element Program, Version 14.0, 2012.

ANSYS, Inc., 2011, *ANSYS Mechanical APDL Element Reference*, November.

AutoCAD, 2D and 3D Design, Drafting, and Modeling Software, 2010.

Berga et al., 2003, *Roller Compacted Concrete Dams*, A.A. Balkema Publishers.

Federal Energy Regulatory Commission, 1999, *Engineering Guidelines for the Evaluation of Hydropower Projects, Chapter 11 Arch Dams*, Division of Dam Safety and Inspections, October.

Idriss, I. M., and Ralph J. Archuleta, 2007, *Engineering Guidelines for the Evaluation of Hydropower Projects, Chapter 13 Evaluation of Seismic Hazards (Draft Version): Evaluation of Earthquake Ground Motions*, Federal Energy Regulatory Commission, Division of Dam Safety and Inspections, February.

James M. Montgomery (JMM), 1983, *Report on Safety Inspection, Salmon Creek Dam, FERC Project No. 2307- Alaska*, February.

MWH, 2007, *Supporting Technical Information, Salmon Creek Hydroelectric Project, FERC Project No. 2307*, November.

Quick Terrain Reader, Photogrammetry Survey Exploitation Software by Applied Imagery, Version 7.1.4, 2011.

United States Army Corps of Engineers, 1997, *ETL 1110-2-542 Thermal Studies of Mass Concrete Structures*, 30 May.

United States Army Corps of Engineers, 1994, *ETL 1110-2-365 Nonlinear, Incremental Finite Element Analysis of Massive Concrete Structures*, 31 August.

United States Bureau of Reclamation, 1981, *A Water Resources Technical Publication, Engineering Monograph No. 34, Control of Cracking in Mass Concrete Structures*, Revised Reprint 1981.

United States Bureau of Reclamation, 2006, *State-of-Practice for the Nonlinear Analysis of Concrete Dams at the Bureau of Reclamation*, January.

Zangar, C.N., 1952, *Hydrodynamic Pressures on Dams Due to Horizontal Earthquake Effects*, U.S. Department of the Interior, Bureau of Reclamation, May.

Zhang, C.; Wolf , J.P., 1998, *Dynamic Soil-Structure Interaction: Current Research in China and Switzerland* , Elsevier Science B.V.